Effects of surface morphology on magnetic properties of Ni nanowire arrays in self-ordered porous alumina

2002 J. Phys.: Condens. Matter 14 715

(http://iopscience.iop.org/0953-8984/14/4/306)

INSTITUTE OF PHYSICS PUBLISHING JOURNAL OF PHYSICS: CONDENSED MATTER

J. Phys.: Condens. Matter **14** (2002) 715–721 PII: S0953-8984(02)28364-2

Effects of surface morphology on magnetic properties of Ni nanowire arrays in self-ordered porous alumina

H Zeng[1], S Michalski[1], R D Kirby[1], D J Sellmyer[1], L Menon[2] and S Bandyopadhyay[2]

[1] Department of Physics and Astronomy, Center for Materials Research and Analysis, University of Nebraska, Lincoln, NE 68588, USA
[2] Department of Electrical Engineering, Center for Materials Research and Analysis, University of Nebraska, Lincoln, NE 68588, USA

Received 29 August 2001, in final form 1 November 2001
Published 18 January 2002
Online at stacks.iop.org/JPhysCM/14/715

Abstract

Ni nanowire arrays were produced by electrodeposition of Ni into self-assembled porous anodic alumina templates. With different anodization voltages, the wires show different surface morphologies. The temperature dependence of the coercivity and activation volume of wires with regular shape can be explained by thermal activation over an energy barrier with a $3/2$ power dependence on the field. The wires with irregular surface morphologies show abnormal temperature dependences of the coercivity and activation volume. Possible mechanisms for these behaviours are discussed.

The magnetization-reversal mechanism of nanowires is an extensively investigated problem [1]. It is well known that coercivity of nanowires mainly arises from the wire shape, which is only weakly dependent on temperature [2]. However, strong temperature dependencies of the coercivity for nanowire systems were reported and attributed to thermal activation processes [3]. Thermal activation is important in the magnetization reversal of nanostructured magnetic materials because of the small size of magnetic entities. Since activation volume is related to the energy barrier to thermally activated reversal, its measurement provides a means to probe the energy barrier function, and therefore the magnetization-reversal process [4, 5].

We have studied the temperature dependencies of the coercivity and activation volume for Ni nanowire arrays embedded in porous alumina. An abnormal temperature-dependent coercivity is observed for wires with irregular surfaces. As far as we know, this interesting behaviour has never been observed before. The temperature-dependent activation volume also shows different behaviours for wires with different morphologies.

The sample preparation procedures were described in [6]. The size and spacing of the nanowires were controlled by anodization voltages and electrolytes. In this study, Al foils were anodized in both 15% sulphuric acid (H_2SO_4) and 3% oxalic acid ($H_2C_2O_4$), and at different voltages. Samples No 1–No 5 correspond to electrolytes and anodization voltages

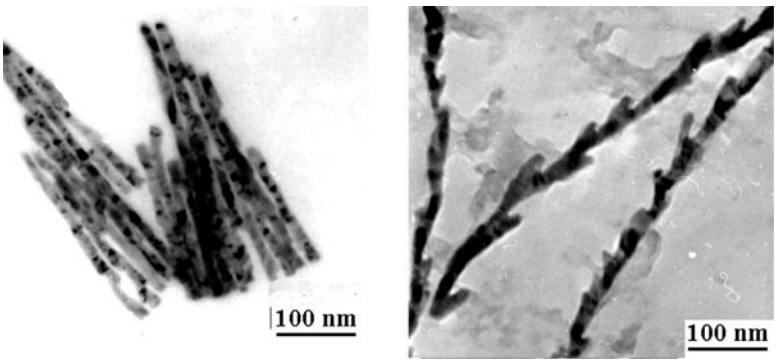

Figure 1. TEM images of Ni nanowires anodized with 15% H_2SO_4 (sample No 2, left) and 3% $H_2C_2O_4$ (sample No 5, right), at 10 V.

as follows: H_2SO_4, 5 V (No 1); H_2SO_4, 10 V (No 2); $H_2C_2O_4$, 20 V (No 3); H_2SO_4, 2 V (No 4); and $H_2C_2O_4$, 10 V (No 5), respectively. The surface morphology of the wires replicates that of the inner walls of the alumina pores. The magnetic properties of the nanowire arrays embedded in the templates were measured by a superconducting-quantum-interference-device (SQUID) magnetometer and a magneto-optic Kerr-effect (MOKE) magnetometer. The field-sweep rate of the MOKE magnetometer is varied from 40 to 2000 Oe s^{-1}, to measure the dynamic coercivity, from which an activation volume (V^*) can be derived. The MOKE signal is proportional to the magnetization to a good approximation, and thus the Kerr rotation as a function of field can be used to measure hysteresis loops. The measurement of V^* involves determining the coercivity as a function of the logarithm of the sweep rate, and the slope is proportional to $k_B T/M_s V^*$ as discussed in [5]. Magnetic measurements were performed with the field perpendicular to the film plane unless otherwise specified.

Figure 1 shows TEM images of nanowires released from the alumina template for samples No 2 and No 5, respectively. The wires are polycrystalline, as can be seen from the dark and bright spots along the wire, representing different crystallographic orientations. Wires of sample No 2 have a nominal diameter of ∼10 nm, and those of sample No 5 have a nominal diameter of ∼20 nm. Besides the difference in diameter, the wires exhibit quite different surface morphologies. For sample No 2, the wires are generally of cylindrical shape, quite uniform in diameter, with more or less smooth surfaces; while for sample No 5, the wires have noticeably irregular shapes. The variation in wire diameter is large; and the wire shape resembles that of a tree with a stem and many short branches.

Generally, nanowires in porous alumina are of cylindrical shape and they resemble wires in sample No 2. However, significant branching, as presented in figure 1, on the right, is observed for low anodization voltages. The threshold voltage, below which significant branching appears, is about 5 V for H_2SO_4 and 10 V for $H_2C_2O_4$. The cause of the branching is not clear, given the complicated pore formation mechanisms [7]. Most probably, below a certain voltage, pores cannot grow and migrate freely, which results in the irregular shape of the pore walls.

It is interesting to see how morphologies affect coercivity and magnetization-reversal behaviours. The samples studied were divided into two groups according to their morphologies. Wires in group 1 (No 1, No 2 and No 3) show regular cylindrical shapes, while those in group 2 (No 4 and No 5) all have irregular surfaces. In order to investigate the compositional homogeneity of the nanowires and any possible variation from group 1 to 2 samples, we have

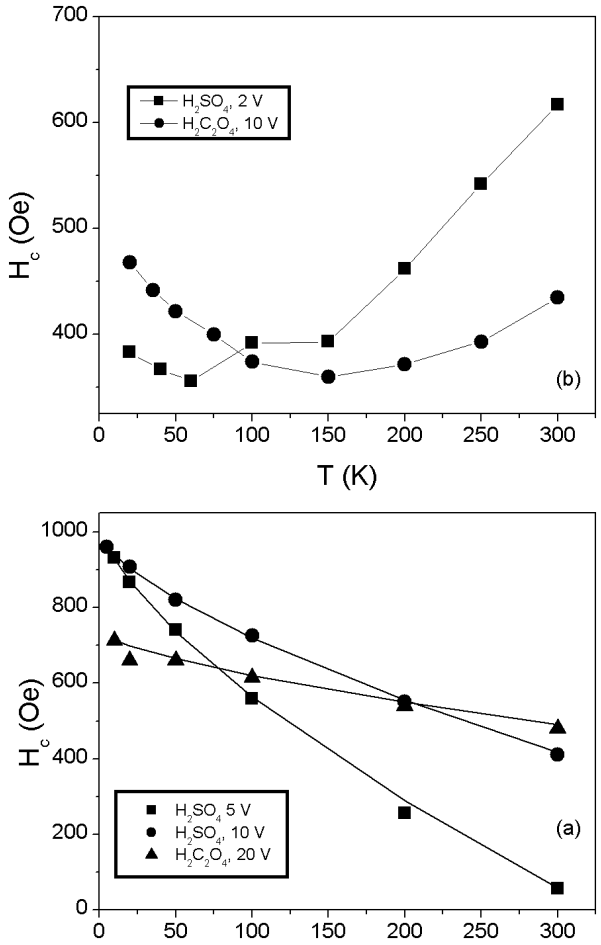

Figure 2. H_c as a function of T as measured by a SQUID for Ni nanowires anodized in (a) H_2SO_4 at 5 V (No 1) and 10 V (No 2) and $H_2C_2O_4$ at 20 V (No 3); the solid curves are fitting curves and (b) H_2SO_4 at 2 V (No 4) and $H_2C_2O_4$ at 10 V (No 5).

performed energy-dispersive x-ray measurements on nanowires released from the templates. The results showed that the composition was homogeneous in a given nanowire, and no differences were found for samples in different groups. Figure 2(a) shows the coercivity (H_c) as a function of temperature (T) measured by the SQUID for group 1 samples. The mean wire diameters are about 5.5, 9 and 39 nm for samples No 1, No 2 and No 3, respectively. It is seen that H_c decreases monotonically with increasing T for all samples. This behaviour is studied in detail in another paper [8]. It is concluded that the temperature dependence is essentially related to the thermally activated magnetization reversal, which initially nucleates within a small volume. The proposed field dependence of the energy barrier for nanowires has the form

$$E_B = E_0(1 - H/H_0)^{3/2} \tag{1}$$

where H_0 is the switching field in the absence of thermal fluctuations, and E_0 is barrier height at zero field. Both H_0 and E_0 mainly arise from the wire shape; therefore $H_0 \propto M_s$ and

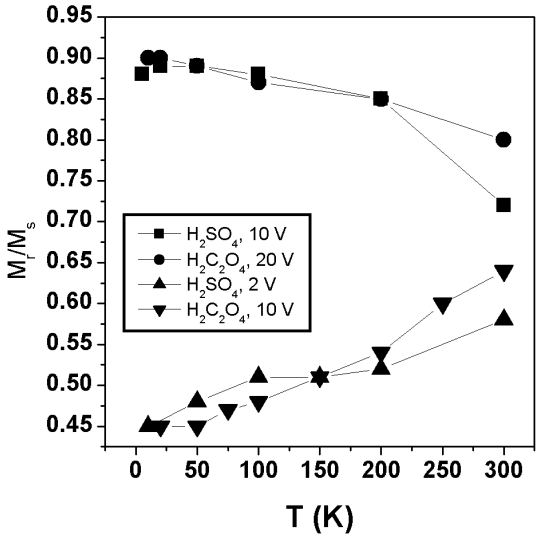

Figure 3. The remanence ratio $S = M_r/M_s$ as a function of T.

$E_0 \propto M_s^2$. The coercivity H_c then follows:

$$H_c(T) = H_{c0}\frac{M_s(T)}{M_{s0}}\left[1 - \left(\frac{25k_BTM_{s0}^2}{E_{00}M_s^2(T)}\right)^{2/3}\right] \tag{2}$$

where H_{c0}, M_{s0} and E_{00} are zero-temperature parameters. It can be seen that equation (2) fits the experimental data very well. The fitted parameters are $H_{c0} = 1050$, 1000 and 720 Oe and $E_{00} = 1.1 \times 10^{-12}$, 2.4×10^{-12} and 5.3×10^{-12} erg, for samples No 1, No 2 and No 3, respectively. These parameters are strongly diameter dependent [8].

In figure 2(b), the fields $H_c(T)$ for samples No 4 and No 5 show surprisingly different behaviour. For both samples, H_c first decreases with increasing T, shows a minimum at around 100 K, and then increases as T increases further. We know that for nanowires with cylindrical shape, the anisotropy is only weakly temperature dependent, and thermal fluctuations only lower H_c with increasing T. Therefore, it is likely that the abnormal $H_c(T)$ behaviour comes from an additional anisotropy which is strongly temperature dependent.

To further investigate the abnormal behaviour, we measured the remanence ratio ($S = M_r/M_s$) as a function of T for both groups. Figure 3 shows that for samples No 2 and No 3, as T decreases, S first increases, then remains nearly constant. This suggests that the easy axis lies along the wire axis for the whole temperature range. The decrease in S at high temperatures may again be due to thermal fluctuations. For group 2 samples (No 4 and No 5), S decreases monotonically with decreasing T. This suggests that the easy axis deviates from the wire axis as T decreases. This is also confirmed by the behaviour of the coercivity and remanence ratio measured parallel to the plane direction. $H_{c\|}$ and $S_\|$ are shown in figures 4(b) and (a), respectively. For samples No 2 and No 3, $H_{c\|}$ remains small and nearly constant throughout the whole temperature range, while $H_{c\|}$ for samples No 4 and No 5 increases monotonically with decreasing T. The $S_\|$-values, as shown in figure 4(a), are small for samples No 2 and No 3, but increase monotonically with decreasing temperature for samples No 4 and No 5, which is similar to the behaviour of $H_{c\|}$.

Therefore, it seems likely that the abnormal $H_c(T)$ behaviour shown in figure 2(b) originates from an additional anisotropy in the lateral direction, which increases monotonically

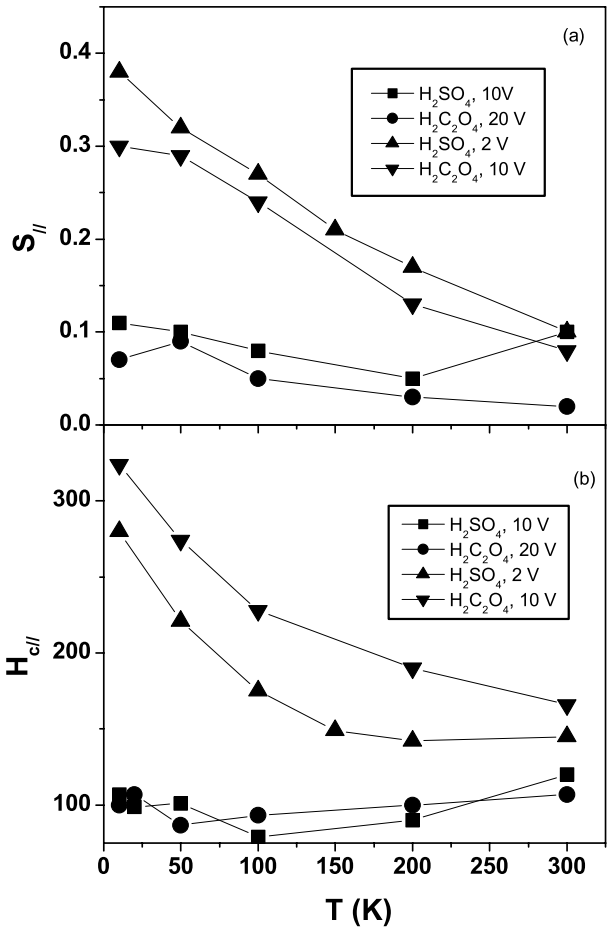

Figure 4. (a) The remanence ratio $S_{\|}$ and (b) the coercivity $H_{c\|}$ as a function of T, both measured in the parallel-to-plane direction.

with decreasing T and tries to align the magnetization perpendicular to the wire axis. At the same time, thermal fluctuations tend to decrease H_c with increasing T; and this competition results in a minimum in $H_c(T)$.

The additional temperature-dependent anisotropy could originate from several factors. The magnetocrystalline anisotropy (K_1) of Ni is strongly temperature dependent, being about 5×10^4 erg cm^{-3} at room temperature and 5×10^5 erg cm^{-3} at 10 K (comparable to the shape anisotropy, $\sim 7 \times 10^5$ erg cm^{-3}). However, Ni nanowires in this study are polycrystalline with no preferential orientations, so the change in K_1 with temperature is not expected to contribute significantly to the total anisotropy change. It also cannot explain why only wires with particular surface morphologies show abnormal behaviours.

Another possibility may be magnetoelastic effects. Previous studies showed that magnetoelastic effects can have profound effects on the magnetic properties of Ni nanowires and depend strongly on nanostructure and preparation conditions [9, 10]. In this case, there is a large mismatch between the thermal expansion coefficients (α) of Ni and alumina. For example, at room temperature, α_{Ni} is $\sim 13.4 \times 10^{-6}$ K^{-1}, while α_{AlO} for recrystallized alumina

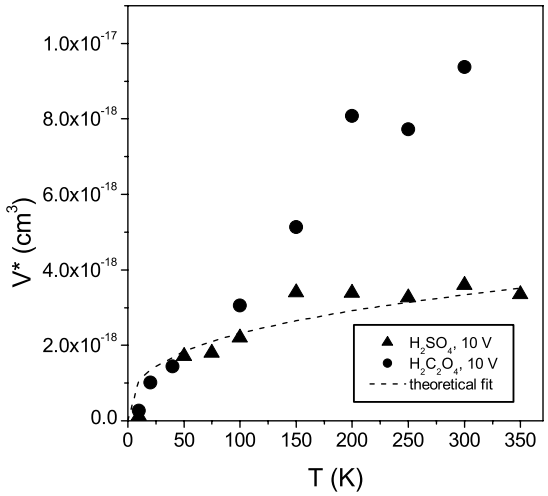

Figure 5. The activation volume V^* as a function of T for samples No 2 and No 5.

is $\sim 6 \times 10^{-6}$ K^{-1}. We expect α for porous alumina to have a similar value. Because of the large difference between α_{Ni} and α_{AlO}, Ni tends to contract more than alumina during cooling. For wires of essentially cylindrical shape, no significant stress is observed, either by us or other groups [11], suggesting that the bonding between the wire and the pore wall is weak. Some evidence even suggests that the wire may detach from the substrate [10]. However, for wires of irregular shape, the relative position of the wire to the pore wall is fixed by numerous branches. Therefore, the wire is forced to contract or expand together with the wall. The mismatch of α can result in an increasing external tensile stress along the wire axis as the temperature is decreased, which may be the origin of the additional magnetoelastic anisotropy.

The magnetoelastic anisotropy can be estimated as follows. The external stress is $\sigma = E\varepsilon$, where E is Young's modulus and ε is the elongation. The magnetoelastic anisotropy is given by

$$K_\sigma = 3/2\lambda_s\sigma \tag{3}$$

where $\lambda_s \approx 34 \times 10^{-6}$ is the isotropic magnetostrictive constant. As a rough estimate, we will use α-values at room temperature to calculate ε:

$$\varepsilon = (\alpha_{\mathrm{AlO}} - \alpha_{\mathrm{Ni}})\Delta T. \tag{4}$$

Ni nanowires are deposited at 60 °C. If we assume $\varepsilon \sim 0$ at 60 °C, then at 100 K, $\Delta T \approx 230$ K. ε as calculated from equation (4) is about -1.7×10^{-3}. Young's modulus E for Ni is about 2.5×10^{12} dyn cm^{-2}; therefore the external stress σ exerted by the template on the Ni nanowire is about 4.25×10^9 dyn cm^{-2}. Finally, as calculated from equation (3), $K_\sigma \approx -2.2 \times 10^5$ erg cm^{-3}. It can be seen that K_σ is of the same order of magnitude as the shape anisotropy ($K_s \approx 7.4 \times 10^5$ erg cm^{-3}), and it increases monotonically with decreasing T. K_σ being negative suggests that the magnetoelastic anisotropy alone will cause the magnetic hard axis to be parallel to the wire axis, and the plane perpendicular to the wire axis to be the easy plane. As a result, with decreasing temperature, magnetoelastic effects will decrease the total anisotropy along the wire axis and therefore the H_c-value.

The activation volume V^* as a function of T was measured for both samples No 2 and No 5, and they are shown in figure 5. It was realized by Gaunt [12] that

$$V^* = -\frac{1}{M_s}\frac{\partial E_B}{\partial H}. \tag{5}$$

For the energy barrier described by equation (1), V^* is easily seen to be

$$V^* = \frac{3}{2}\frac{E_0^{2/3}(25k_BT)^{1/3}}{M_sH_0} = \frac{3}{2}\frac{E_{00}^{2/3}M_{s0}^{2/3}(25k_BT)^{1/3}}{M_s^{5/3}H_{c0}}. \tag{6}$$

It is seen in figure 5 that V^* for No 2 agrees reasonably well with this prediction. Since both H_c and V^* are determined by the energy barrier, the fitting from both equations (2) and (6) should give the same E_{00}-value if our model is self-consistent. E_{00} obtained from fits to equation (2) is 1.1×10^{-12} erg cm^{-3}, while that from equation (6) is 1.12×10^{-12} erg cm^{-3}, which are very close. For No 5, V^* as a function of T is nearly linear; nonetheless, the interpretation is nontrivial. Because of the unique morphology, every branch could act as a nucleation site; therefore the magnetization reversal could be dominated by numerous nucleation processes. It is not likely that a single-energy-barrier picture can be used to describe such systems.

In summary, the coercivity as a function of temperature for nanowires with near-ideal morphologies is consistent with an energy barrier that varies as $(H - H_0)^{3/2}$, while nanowires with branched features show an abnormal increase in coercivity with increasing temperature. This latter behaviour may be attributed to magnetoelastic effects. The temperature-dependent activation volume for near-ideal wires is consistent with the proposed energy barrier.

Acknowledgments

The authors would like to thank S Liou and R Sabiryanov for stimulating discussions. This research was supported by the US Army Research Office, the Nebraska Research Initiative, the Center for Materials Research and Analysis and IBM.

References

[1] See e.g. Sellmyer D J, Zheng M and Skomski R 2001 *J. Phys.: Condens. Matter* **13** R433 and references therein
[2] Al-Mawlawi D, Coombs N and Moskovits M 1991 *J. Appl. Phys.* **70** 4421
[3] Wernsdorfer W, Hasselbach K, Benoit A, Doudin B, Meier J, Ansermet J-Ph and Mailly D 1997 *Phys. Rev.* B **55** 11 552
[4] Lyberatos A and Chantrell R W 1997 *J. Phys.: Condens. Matter* **9** 2623
[5] Kirby R, Yu M and Sellmyer D J 2000 *J. Appl. Phys.* **87** 5696
[6] Zeng H, Zheng M, Skomski R, Sellmyer D J, Liu Y, Menon L and Bandyopadhyay S 2000 *J. Appl. Phys.* **87** 4718
[7] Li F Y 1998 *PhD Dissertation* University of Alabama
[8] Zeng H *et al* 2001 *Phys. Rev.* B submitted
[9] Dubois S, Colin J, Duvail J L and Piraus L 2000 *Phys. Rev.* B **61** 14 315
[10] Jorritsma J and Mydosh J A 1998 *J. Appl. Phys.* **84** 901
[11] Huysmans G T A, Lodder J C and Wakui J 1988 *J. Appl. Phys.* **64** 2016
[12] Gaunt P 1986 *J. Appl. Phys.* **59** 4129